Thermochemical production of liquid fuels from biomass: Thermo-economic modeling, process design and process integration analysis

Laurence Tock Martin Gassner, François Maréchal

Industrial Energy Systems Laboratory, Ecole Polytechnique Fédérale de Lausanne
CH – 1015 Lausanne, Switzerland

Abstract

A detailed thermo-economic model combining thermodynamics with economic analysis and considering different technological alternatives for the thermochemical production of liquid fuels from lignocellulosic biomass is presented. Energetic and economic models for the production of Fischer-Tropsch fuel (FT), methanol (MeOH) and dimethyl ether (DME) by the means of biomass drying with steam or flue gas, directly or indirectly heated fluidized bed or entrained flow gasification, hot or cold gas cleaning, fuel synthesis and upgrading are reviewed and developed. The process is integrated and the optimal utility system is computed. The competitiveness of the different process options is compared systematically with regard to energetic, economic and environmental considerations. At several examples, it is highlighted that process integration is a key element that allows for considerably increasing the performance by optimal utility integration and energy conversion. The performance computations of some exemplary technology scenarios of integrated plants yield overall energy efficiencies of 59.8% (crude FT-fuel), 52.5% (MeOH) and 53.5% (DME), and production costs of 89, 128 and 113 $\in \cdot MWh^{-1}$ on fuel basis. The applied process design approach allows to evaluate the economic competitiveness compared to fossil fuels, to study the influence of the biomass and electricity price and to project for different plant capacities. Process integration reveals in particular potential energy savings and waste heat valorization. Based on this work, the most promising options for the polygeneration of fuel, power and heat will be determined in a future thermo-economic optimization.

Keywords: Biofuels, Biomass, Process design, Process integration, Thermo-economic modeling, Thermal optimization

Nomenclature

Abbreviations
BtL   Biomass to Liquid
CFB   Circulating Fluidized Bed
CGCL Cold Gas Cleaning
DME   Dimethyl Ether
EF   Entrained Flow
FICFB Fast Internally Circulating Fluidized Bed
FT   Fischer-Tropsch
GCL   Gas Cleaning
GT   Gas Turbine
HGCL Hot Gas Cleaning

HP	Heat Pump	
HTFT	High Temperature Fischer-Tropsch process	
LTFT	Low Temperature Fischer-Tropsch process	
MEA	Monoethanolamine	
MeOH	Methanol	
SAS	SASOL Advanced Synthol	
SMR	Steam Methane Reforming	
SNG	Synthetic Natural Gas	
WGS	Water-Gas Shift	

Greek letters

α	Growth probability	-
Δh^0	Lower heating value	$kJ \cdot kg^{-1}$
$\Delta \tilde{h}_r{}^0$	Standard heat of reaction	$kJ \cdot mol^{-1}$
ϵ_{chem}	Chemical efficiency	%
$\epsilon_{murphree}$	Murphree efficiency	%
ϵ_{tot}	Overall energy efficiency	%
Δk^o	Exergy value	$MJ \cdot kg^{-1}$
Φ	Humidity	$kg_{H2O} \cdot kg_{tot}^{-1}$

Roman letters

d	Diameter	m
$\dot{E}$	Mechanical/electrical power	kW
h	Height	m
K_P	Equilibrium constant	variable
$\dot{m}$	Mass flow	$kg \cdot s^{-1}$
N	Number of plates of distillation column	-
P	Pressure	MPa
P_n	Mole fraction of hydrocarbon molecules containing n carbon atoms	%
$\dot{Q}$	Heat	kW
R	Ideal gas constant	$J \cdot K^{-1} \cdot mol^{-1}$
T	Temperature	°C or K
T_{cor}	Corrected Temperature	K
u_{mean}	Mean gas velocity	$m \cdot s^{-1}$
$\dot{V}$	Volumetric flowrate	$m^3 \cdot s^{-1}$
$vol\%$	Volume percent	%
$wt\%$	Weight percent	%

Superscripts

| $^+$ | Material or energy stream entering the system |
| $^-$ | Material or energy stream leaving the system |

1 Introduction

With the steadily increasing energy consumption contributing to the depletion of fossil resources, the insecurity of energy supply and global warming, renewable energy resources emitting less CO_2 become popular alternatives to substitute fossil fuels, especially in the transportation sector which is responsible for a large part of the global CO_2 emissions. A promising renewable and widely available resource is biomass having many applications as energy source generating heat, electricity and transportation fuels with low lifecycle CO_2 emissions.

Worldwide R&D efforts focus currently on the conversion of biomass to liquid fuels (BtL). The review and the evaluation of technologies suitable for biomass gasification presented in the ETPC report (Olofsson et al., 2005), indicate that it is technically feasible and that basic principles are well developed, but concludes that some technical challenges regarding process

economy and operation have to be overcome for a successful commercial implementation of these processes. The extensive literature review made in (Spath and Dayton, 2003) summarizes the operating conditions and the technological, environmental and economic aspects of some syngas conversion processes based on experimental data from existing installations.

High-efficiency technology for the sustainable use of biomass in the conversion of energy, fuel and products is assessed by the Energy research Centre of the Netherlands (ECN, Last visited 07/2009). The technical and economic performance of biomass to Fischer-Tropsch liquids conversion concepts modeled and evaluated in (Hamelinck et al., 2004) yield an overall efficiency of 40 to 45% based on the higher heating value basis. In (Hamelinck and Faaij, 2002), the technical and economic evaluation of the promising process for producing methanol yield an overall efficiency around 55% based on the higher heating value. In these studies, the performance is evaluated using flowsheeting models, and process economics have been estimated by capacity-based correlations disregarding the specific process conditions. Only limited energy integration has been performed and cogeneration possibilities have not been assessed in detail. By developing detailed thermo-economic models for the performance computation and energy integration according to the methodology applied in (Gassner and Maréchal, 2009b), the competitiveness of the different biomass conversion processes could be systematically investigated in a consistent way.

The purpose of the present work is to develop models that allow one to analyze technological alternatives for the thermochemical conversion of biomass into different types of liquid fuels, mainly Fischer-Tropsch crude fuel, dimethyl ether and methanol and by applying a systematic methodology comprising the definition of a process superstructure, the use of process integration techniques and economic analysis considering specific process designs (Maréchal et al., 2005). This methodology is appropriate for the conceptual process design that identifies the promising system configurations. In this paper, the process integration of existing technologies and its influence on the energy efficiency is highlighted, especially by revealing the potential of the optimal energy conversion and the combined heat and power production. The presented work constitutes the basis for a future thermo-economic process optimization (Gassner and Maréchal, 2009a) including environmental indicators (Gerber et al., 2009).

2 Design Methodology

After the assessment of candidate process technologies defined from the literature, the process flow superstructure including all possible options is defined. In the thermo-economic model (i.e.thermodynamics and economics) separate energy-flow, energy-integration and economic models are developed, following the methodology outlined in (Gassner and Maréchal, 2009a).

In the energy-flow models, the occurring chemical and physical transformations are calculated and their heating, cooling and mechanical power requirements are determined by applying mass and energy balances based on the laws of thermodynamics using conventional flowsheeting tools. The hot and cold streams are then integrated in the energy-integration model, where the balance of plant, the combined heat and power production and the heat recovery system is computed. Considering the material flows defined in the process superstructure and the heat cascade as constraints, the combined production of fuel, power and heat is thereby optimized with regard to minimal operating cost (Gassner and Maréchal, 2009a; Maréchal and Kalitventzeff, 1998). In the economic model, the process equipment is preliminarily sized in order to meet the thermodynamic targets set by the flowsheet model, and the investment cost is estimated with correlations from the literature (Turton, 2009; Ulrich and Vasudevan, 2003).

The purpose of the thermo-economic modeling is to compute the systems' performance as a function of the decision variables (i.e. technology choices and operating conditions) and to identify the critical parameters and the opportunities for process improvements by considering

the various combinations between different process options. The developed models are flexible and robust. They allow for computing the performances at different plant capacities since their thermodynamic part is scale-independent.

3 Process Description

3.1 Process Block Flow Superstructure

The main steps of the thermochemical conversion of lignocellulosic biomass into liquid fuels are feed conditioning, gasification, gas cleaning (GCL), reforming of hydrocarbons, shift and gas separation for stoichiometry adjustment for the fuel synthesis and fuel purification. The different technological options of each step, as well as the recycling options are summarized in Figure 1. The process layout is similar to the one developed in (Gassner and Maréchal, 2009b) for the syngas production [1] and in (Hamelinck et al., 2004; Hamelinck and Faaij, 2002; Ogawa et al., 2003) for FT, MeOH and DME synthesis respectively. The investigated alternatives assembled by dashed lines in Figure 1 for the main process steps are described in the following Section 3.2.
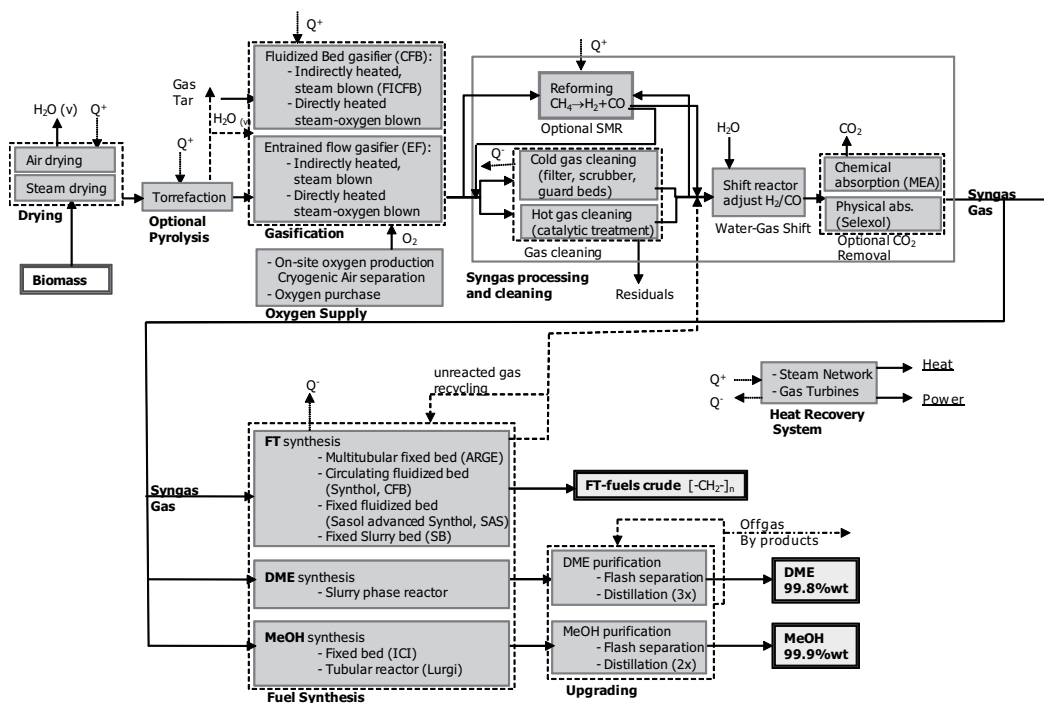

Figure 1: Process Superstructure. Dashed lines assemble investigated alternatives for the corresponding process steps.

3.2 Process Technologies

The technologies considered in the superstructure presented in Figure 1 are widely described in literature (Olofsson et al., 2005; Spath and Dayton, 2003; Hamelinck et al., 2004; Hamelinck and Faaij, 2002; Gassner and Maréchal, 2009b; Tijmensen et al., 2002; Kaneko et al., 2001).

---

[1]Syngas or synthesis gas is a mixture consisting primarily of hydrogen and carbon monoxide. The syngas produced by the gasification of biomass consists mainly of H_2, CO, CO_2 and CH_4; because of the presence of CH_4 this is sometimes referred to as producer gas (Gassner and Maréchal, 2009b), however according to Wyer (1907) producer gas contains a high level of N_2.

Pretreatment and gasification   Drying, pyrolysis and gasification are endothermal processes requiring heat supply, either by external heating or by supplying sufficient oxygen to oxidize part of the product. Different gasification methods, including atmospheric and pressurized, steam-blown, and oxygen-steam-blown, indirectly and directly heated entrained flow (EF) or fluidized bed (FICFB, CFB) gasification, are considered for the production of syngas characterized by specific H_2/CO ratios. For the entrained flow gasification a torrefaction step is required in order to pulverize the raw material. A detailed technology description, as well as the advantages and disadvantages of the different gasifiers are reported in (Olofsson et al., 2005). The oxygen required for the directly heated gasification can either be purchased or produced on-site through air separation by cryogenic distillation or pressure swing adsorption or alternatively membrane processes (Kirschner, 2000).

Gas cleaning and treatment   Prior to fuel synthesis, part of the contaminants contained in the syngas has to be removed by either hot (HGCL) or cold (CGCL) gas cleaning as described in (Olofsson et al., 2005; Hamelinck et al., 2004; Hamelinck and Faaij, 2002). The gas composition is then adjusted to match the needs of the reactant stoichiometry for the subsequent synthesis reactions by steam methane reforming (SMR), water-gas shift reaction (WGS) and/or CO_2 removal. The technologies considered for CO_2 removal are chemical absorption with monoethanolamine (MEA) and physical absorption (Selexol process) (Radgen et al., 2005). Other alternatives would be adsorption or permeation processes.

Fuel synthesis   Different types of liquid fuels can be synthesized from the syngas. The characteristics of the synthesis reactions and the corresponding reactors technologies are reported in Table 1.

The **Fischer-Tropsch** synthesis process consists in a catalytic non-selective exothermal reaction (Eq.2) in which syngas is converted into hydrocarbons of different lengths according to an Anderson-Schulz-Flory distribution (Eq.14) expressing the mole fraction P_n of hydrocarbon molecules containing n carbon atoms as a function of the growth probability α (Kaneko et al., 2001). α expresses the chance that a hydrocarbon chain grows with another CH_2 instead of terminating.

$$P_n = \alpha^{n-1}(1 - \alpha) \tag{14}$$

FT synthesis reactors that are commonly operated are: multitubular fixed-bed reactors and slurry bed reactors for the low-temperature FT processes (LTFT: T=220-250°C, P=2.5-4.5MPa and CO or Fe catalyst) and circulating fluidized bed reactors and fixed fluidized bed reactors for the high-temperature FT processes (HTFT: T=330-350°C, P=2.5MPa and Fe catalyst) (Olofsson et al., 2005; Spath and Dayton, 2003).

The **DME synthesis** proceeds by an exothermal reaction producing DME from MeOH (Eq.5). Two reaction routes from syngas can be distinguished: the classical two step route (Eq.7) where the formation of methanol proceeds in an autothermal reactor and the methanol dehydration in a separate fixed bed reactor, and the direct one-step synthesis of DME from syngas (Eq.6) performed in a single slurry phase reactor stage (Olofsson et al., 2005; Ogawa et al., 2003).

Methanol is synthetically produced by exothermal catalytic equilibrium reactions involving the conversion of carbon oxides and hydrogen (Eq.8 & Eq.9). Conventional methanol reactors are adiabatic reactors with cold unreacted gas injected between the catalyst beds and quasi-isothermal reactors with shell and tube design (Spath and Dayton, 2003; Hamelinck and Faaij, 2002; Fiedler et al., 2000).

5

Table 1: Chemical reactions occurring in the process.

Name	Reaction	$\Delta \tilde{h}_r{}^0 \ [kJ \cdot mol^{-1}]$	Reactor
Alcohols formation	$nCO + 2nH_2 \rightarrow C_nH_{2n+1}OH + (n-1)H_2O$		FT
			(1)
FT chain growth reaction	$CO + 2H_2 \rightarrow -CH_2- + H_2O$	-165	FT
			(2)
Olefins formation	$2nH_2 + nCO \rightarrow C_nH_{2n} + nH_2O$		FT
			(3)
Paraffins formation	$(2n+1)H_2 + nCO \rightarrow C_nH_{2n+2} + nH_2O$		FT
			(4)
Methanol dehydration	$2CH_3OH \rightleftharpoons CH_3OCH_3 + H_2O$	-23.4	$DME, MeOH$
			(5)
One-step DME synthesis	$3CO + 3H_2 \rightleftharpoons CH_3OCH_3 + CO_2$	-246.5	DME
			(6)
Two-step DME synthesis	$2CO + 4H_2 \rightleftharpoons CH_3OCH_3 + H_2O$	-205	DME
			(7)
Methanol synthesis	$CO + 2H_2 \rightleftharpoons CH_3OH$	-90.8	$MeOH, DME$
			(8)
	$CO_2 + 3H_2 \rightleftharpoons CH_3OH + H_2O$	-49.16	$MeOH$
			(9)
Ethanol formation	$2CH_3OH \rightleftharpoons C_2H_5OH + H_2O$	-71.8	$MeOH$
			(10)
Steam methane reforming	$CH_4 + H_2O \rightleftharpoons CO + 3H_2$	206	SMR
			(11)
Ethene reforming	$C_2H_4 + 2H_2O \rightleftharpoons 2CO + 4H_2$	210	SMR
			(12)
Water-gas shift equilibrium	$CO + H_2O \rightleftharpoons CO_2 + H_2$	-41	SMR, WGS
			(13)
			$DME, MeOH$

4 Process Modeling

4.0.1 Thermodynamic Model

In the flowsheet modeling different thermodynamic models are used to calculate the liquid-vapor and chemical equilibrium. For the pretreatment units and the production of the syngas, ideal gas behavior has been selected. Ideal behavior is also assumed for the FT-crude process streams because of the presence of hydrocarbons. However, for the synthesis and purification units of the DME and MeOH routes the effects of binary interactions should be considered. The liquid and vapor phase behavior is predicted by the Peng-Robinson equation of state. The corresponding parameters of the Peng-Robinson model are obtained from DECHEMA Chemistry Data Series (Gmehling and Onken, 2005, 1988; DECHEMA, Last visited 07/2009) (Supplementary material Table 12).

The thermodynamic model used to calculate the interaction properties in the purification section is the activity coefficient model UNIQUAC for the methanol process and the NRTL model for the DME process. The parameters for each model are adapted from the DECHEMA Chemistry Data Series (DECHEMA, Last visited 07/2009) (Supplementary material Tables 13, 14 & 15).

4.1 Energy-Flow Models

The energy-flow models define the chemical and physical transformations through the units of the superstructure and define the heat transfer requirements. These models require to be robust enough to evaluate different process configurations, and precise enough to represent the performance of the process units.

The models for the biomass pretreatment, gasification and gas cleaning used in this study are identical to those developed for the production of SNG described in (Gassner and Maréchal, 2009b). In this work, only the specific technology models required for the BtL routes are discussed. The common basic assumptions and key parameters are summarized in Tables 2, 3 and 4. The chemical reactions used in this paper were already presented in Table 1.

Table 2: Parameters and assumptions for the energy-flow models of the syngas production and treatment units adapted from (Gassner and Maréchal, 2009b).

Section	Specification	Value
Wood feedstock	Composition (weight fractions)	C=51.09%, H=5.75%
		O=42.97%, N=0.19%
	Wood inlet humidity	50%
Pyrolysis	Temperature	260°C
	Wood inlet humidity	25%
O_2 production (Hamelinck et al., 2004)	Energy consumption	$300 \ kWh \cdot (to \ of \ O_2)^{-1}$
Gas cleaning	Filter inlet temperature	150°C
	Filter pressure drop	10kPa
	Flash temperature	25°C
Water gas shift	H_2/CO ratio	from theoretical stoichiometry
CO_2 removal by MEA	Thermal Load @ 150°C	$3.7 MJ \cdot kg^{-1} \ CO_2$
absorption (95% efficiency) (Radgen et al., 2005)	Electric Power	$1.0 MJ \cdot kg^{-1} \ CO_2$
Physical absorption	CO_2-solubility in Selexol	$1.8 \ mol \cdot l^{-1} \cdot MPa^{-1}$
	Relative solubility CO_2/CH_4	17.1
	Regeneration pressure	0.1 MPa

4.1.1 Gasification and Steam Methane Reforming

The syngas produced by fluidized bed gasifiers operating below 1000°C is generally not in equilibrium, and consequently their modeling is done by adjusting the equilibrium relationships to the observed gas composition. In (Gassner and Maréchal, 2009b), temperature differences to

equilibrium are used and the reaction extent is specified by a constant carbon conversion. The fluidized bed gasifiers are modeled in this work by applying this modeling approach with the same values for the key parameters. For entrained flow gasifiers operating at higher temperatures, the reaction kinetics are generally sufficiently fast that thermodynamic equilibrium can be assumed. A torrefaction step is included before the gasification to break the dried feedstock down into a gaseous, liquid and solid part and so to dry the biomass further. Such a step is required for EF gasification to pulverize the feed and could optionally be included in the other process configurations. Table 3 summarizes the gasification operating conditions for the different scenarios investigated in this work.

Table 3: Operating conditions of the investigated gasification technologies

Technology	FICFB	CFB	EF	EF
	indirectly heated	directly heated	directly heated	indirectly heated
Gasification P [MPa]	0.1	3	3	3
Gasification T [°C]	850	850	1350	1350
Steam preheat T [°C]	400	400	400	400
Steam to biomass ratio [-]	0.5	0.6	0.6	1

The steam methane reforming performed after the gasification to convert the remaining hydrocarbons into hydrogen and carbon monoxide, is modeled by considering the reactions Eq.11, Eq.12 and Eq.13 (Table 1) at equilibrium. The steam to carbon ratio influencing the reaction equilibrium is fixed through the amount of steam used in the gasification. The reforming temperature is a decision variable that will be calculated to optimize the process performance (See Section 5.2.4).

4.1.2 Liquid Fuel Synthesis and Upgrading

The operating conditions and the key decision variables for the developed Fischer-Tropsch fuel (FT), dimethyl ether (DME) and methanol (MeOH) process models are summarized in Table 4.

FT synthesis The FT synthesis is described by the chain growth reaction (Eq.2), whose chain termination mechanisms generally results in the formation of olefins (alkenes) (Eq.3), paraffins (alkanes) (Eq.4) and alcohols (Eq.1). For the modeling, only the formation of olefins and paraffins is considered, whose distribution in the C_2-C_4, C_5-C_{12} and C_{13}-C_{18} hydrocarbon ranges is adjusted according to the data reported in (Kaneko et al., 2001; Jager and Espinoza, 1995). This leads to the production of a crude FT fuel to be further processed in an oil refinery.

Important parameters for the FT productivity are the reactor type and size, the operating conditions, the CO-conversion (Eq.2), the growth probability α defining the product distribution (Eq.14) and the product selectivity. The modeling parameters are calibrated on data from Kaneko et al. (2001); Jager and Espinoza (1995) for a one-pass process with fluidized bed technology (Sasol Advanced Synthol (SAS) fluidized bed) and cobalt-catalysis at 340°C. For this technology a value of α=0.884 is reconciled with the reported hydrocarbon distribution. This value results in a mean deviation of less than 0.7% and complies with the typical selectivities of 0.78 to 0.82 reported for classical Co-catalysts and 0.8 to 0.94 for new catalysts reported by (Jager and Espinoza, 1995). The variation of the selectivity with the operating conditions described in (Hamelinck et al., 2004), is not taken into account in this model, since numerical values of the different parameters are not available for different reactors and catalysts.

The size of the reactor is estimated based on an empiric relation between the diameter d, the volumetric flowrate $\dot{V}$ and the mean gas velocity u_{mean} (Eq.15), and an exponential relation between the height h and the volumetric flowrate $\dot{V}$ (Eq.16). The numerical values are calibrated using literature data (Fox et al., 1990) and reported in Table 5.

Table 4: Parameters and assumptions for the energy-flow models of the synthesis units.

Section	Specification	Value
FT synthesis	T	340°C
	P	2.5 MPa
	Stoichiometry: $\frac{H_2}{CO}$ ratio	2
	Growth probability α	0.884
	Olefinic fractions (rest paraffinic):	
	C_2-C_4	0.8
	C_5-C_{12}	0.7
	C_{13}-C_{18}	0.6
	CO-conversion	85%
DME synthesis	T	277°C
	P	5 MPa
	Stoichiometry: $\frac{H_2}{CO}$ ratio	1.3
	CO_2 removal after gas cleaning	95%
	Unreacted gas recycling	80%
	Methanol Dehydration ΔT	5°C
MeOH synthesis	T	260 °C
	P	8.5 MPa
	Stoichiometry: $\frac{H_2-CO_2}{CO+CO_2}$ ratio	2
	CO_2 removal	fixed by $\frac{H_2-CO_2}{CO+CO_2}=2$
	Unreacted gas recycling	90%
	Methanol Synthesis ΔT	3.6°C
	By-products selectivity	0.8%

$$d = 2\sqrt{\frac{\dot{V}}{\Pi \cdot u_{mean}}} \qquad [m] \tag{15}$$

$$h = h_o \dot{V}^b \qquad [m] \tag{16}$$

Table 5: Sizing parameters for the synthesis reactors.

Process	u_{mean} [m·s^{-1}]	h_0 [m·$(m^3 \cdot s^{-1})^{-b}$]	b
FT-crude (Fox et al., 1990)	0.136	2	1.158
DME (Ohno, 2001)	0.2	21.77	0.073
MeOH (Fox et al., 1990)	0.317	h/d=1.62	-

FT upgrading The separation and purification by hydrotreating, hydrocracking and hydroisomerization of the crude FT product is not included in this work, and only the separation of water and unreacted gas in a flash drum is considered in the model. The final product is therefore crude FT-fuel which can be sent to a refinery for upgrading.

DME synthesis The modeling of the DME synthesis is based on the one-step process (Eq.6) operated in a slurry phase reactor where the water-gas shift reaction (Eq.13), the methanol synthesis from syngas (Eq.8) and the methanol dehydration reaction (Eq.5) take place.

The methanol dehydration reaction (Eq.5) is assumed to be at equilibrium with an equilibrium temperature difference taking into account the deviation from the equilibrium conditions. The selected operating conditions reach a temperature of 277°C and a pressure of 5MPa at the outlet of the reactor. A deviation of $\Delta T_{MeOH,dehyd.}=5$°C from the equilibrium temperature is assumed. The water-gas shift reaction (Eq.13) is expected to be at equilibrium and the methanol

9

synthesis (Eq.8) is considered as a conversion reaction whose extent is specified with a relation setting the ratio between the extent of equation (Eq.5) and (Eq.8) to 47%, which is based on the stoichiometry relation between the two reactions (factor of 1/2).

The size of the DME reactor is calculated using the diameter (Eq.15) and height (Eq.16) estimations and the numerical values calibrated using the numerical data from literature (Ohno, 2001) reported in Table 5.

DME upgrading   At the DME reactor outlet a flash drum separates part of the unreacted gases from the product stream. The unreacted gas is recycled partly towards the reactor to increase the efficiency. High purity DME is obtained after a second flash drum and three distillation steps. The distillate of the first distillation step consisting essentially of light gases is combusted for heat and power generation in this study, but could optionally be recycled in the process. The modeling of the DME upgrading illustrated in Figure 2 is based on a purity requirement of 99.8 wt% DME for which the characteristic parameters are reported in Table 6.
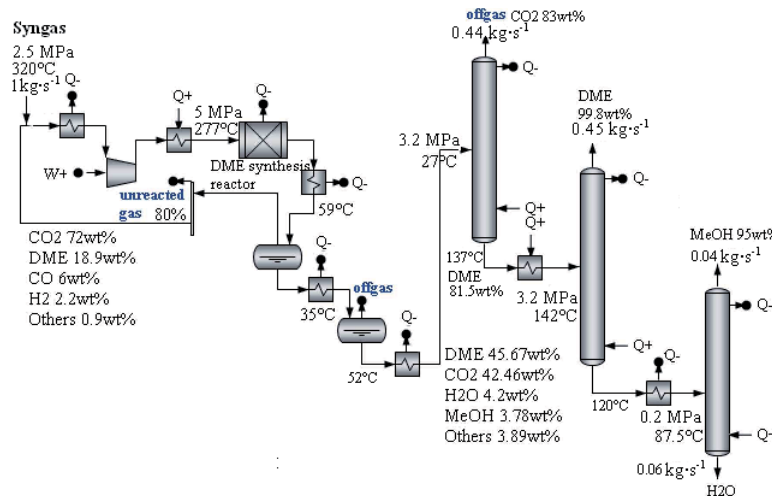

Figure 2: Flowsheet of the DME synthesis and upgrading for a normalized syngas stream of 1 $kg \cdot s-1$ at the inlet

.

Table 6: Parameters of the DME and MeOH purification models.

Parameter	DME process			MeOH process	
	1st dist.	2nd dist.	3rd dist.	1st dist.	2nd dist.
$\epsilon_{murphree}$	85%	85%	85%	85%	85%
N^o plates	8	11	16	22	45
Feed plate	1	5	5	11	20
Reflux ratio	0.7	0.7	2.6	1.3	1.3
Inlet T [°C]	27	142	87.5	115	85
Inlet P [MPa]	3.2	3.2	0.2	0.8	0.2
Purity [wt%]	DME: 81.5	DME: 99.8	MeOH: 95	MeOH: 99	MeOH: 99.9

Methanol synthesis   The modeling of the methanol synthesis considers a multistage reactor containing four beds as described in (Maréchal et al., 1997). The applied reaction scheme considers the reverse water-gas shift reaction (Eq.13), the methanol synthesis from syngas (Eq.9) and the formation of the by-products DME (Eq.5) and ethanol (Eq.10).

The methanol synthesis (Eq.9) is modeled by an equilibrium reaction with an equilibrium temperature difference $\Delta T_{MeOH,syn.}$ of 3.6°C in order to take a deviation of 95% from the

10

equilibrium conversion at 260°C and 8.5MPa into account. The water-gas shift reaction (Eq.13) is expected to be at equilibrium while the by-products formation (Eq.10 & Eq.5) is modeled as conversion a reaction whose extent is specified by the selectivity for the ethanol and DME production fixed to 0.8% as reported in (Grambezen, -).

The methanol reactor diameter is calculated by Eq.15 and the height is estimated by fixing the ratio h/d to 1.62 based on literature data (Fox et al., 1990) reported in Table 5.

MeOH upgrading As for the DME upgrading the unreacted gas is first separated in a flash drum and recycled to the reactor or burned, as depicted in Figure 3. A purity of 99.9 wt% MeOH is reached after two distillation steps characterized by the parameters reported in Table 6.
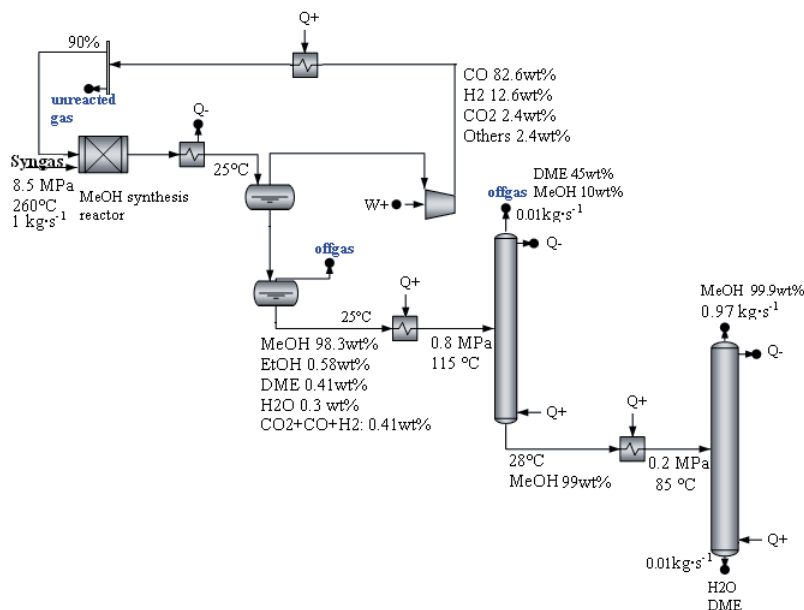

Figure 3: Flowsheet of the MeOH synthesis and upgrading for a normalized syngas stream of 1 $kg \cdot s-1$ at the inlet

.

4.2 Energy-integration Model

Energy integration consists in minimizing the energy consumption of a process by calculating thermodynamically feasible energy targets and achieving them by optimizing the heat recovery, energy conversion and the process operating conditions. As detailed in (Gassner and Maréchal, 2009a; Maréchal and Kalitventzeff, 1998), the energy integration model is based on the definition and the identification of the hot and cold streams temperature enthaply profiles and their minimum approach temperature $\Delta T_{min}/2$. $\Delta T_{min}/2$ values of 8, 4 and 2K are assumed for gaseous, liquid and condensing/evaporating streams, respectively. The integrated composite curve of Figure 4 illustrates for example, the steam network integration of the FT-crude process in the corrected temperature domain (T_{cor}). In all the reported enthaply-temperature profiles the heat loads are normalized per MW of biomass processed in the system.

Below the gasification temperature, heat is recovered from the hot syngas, the reforming and the purification section where the gas stream is cooled down. Heat is also released by the exothermal synthesis reaction and required by the endothermal pyrolysis reaction, to heat the
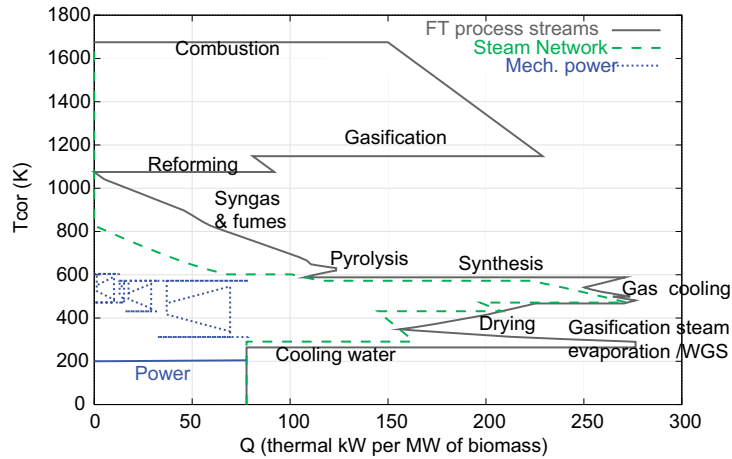
11

Figure 4: Typical integrated composite curve including a steam network for the FT-crude process with FICFB gasification.

water prior to evaporation and to reheat the steam for gasification. A considerable amount is also consumed at lower temperature for biomass drying. There is hence a steam demand from the dryer, the gasifier, the reformer and the shift reactor. After heat recovery the energy balance shows an excess of heat that can be converted partly into mechanical power before being released to the environment. Furthermore, the introduction of a heat pump (HP) can be advantageous in order to valorize the exergy potential of the high temperature heat by conversion into electricity. The heat that has to be supplied above the high temperature pinch point is generated by the combustion of different waste streams of the process, like dried torrified gases, char and/or offgases from distillation. If necessary, the balance is closed by using intermediate product streams from the process such as the gas stream after gasification (hot gas) or after gas cleaning (cold gas) as a process fuel.

The integration of these options is addressed in detail in Section 5.2.

4.3   Economic Model

The economic evaluation of the investment is based on the size and the type of construction material of each equipment that depends on the process productivity determined by the decision variables and operating conditions. The equipments' size is defined based on the physical quantities computed from the flowsheet models. The dimensions of the dryers, the torrifaction reactor, the gasifiers and the gas cleaning units are estimated with the data reported in (Gassner and Maréchal, 2009b) while the synthesis reactor sizing was discussed in Section 4.1.2.

Following the approach outlined in (Turton, 2009), the costs of the equipments are estimated from the capacity-based correlations given in (Turton, 2009; Ulrich and Vasudevan, 2003). The production costs are evaluated by dividing the total annual costs of the system consisting of annual investment, operating and maintenance, raw material and electricity supply/demand, by the produced amount of fuel. Furthermore, a biomass break-even cost expressed in € per MWh of biomass, that defines the maximum resource price for which the process is profitable, is calculated from the electricity and fuel sale price reported in Table 7. All the costs have been updated to year 2007 by using the Marshall Swift Index. The different assumptions for the economic analysis are summarized in Table 7.

The sizing and cost estimation method for shell and tube reactors with catalysts reported in (Maréchal et al., 2005) is applied for the reforming reactor with a Ni/Al_2O_3 catalyst and for the WGS reactor with a Pd/Al_2O_3 catalyst. The distillation column costs are estimated by design heuristics for packed towers (Ulrich and Vasudevan, 2003) based on the number of plates and

12

Table 7: Assumptions for the economic analysis.

Parameter	Value
Marshall and Swift index (2007)	1399
Dollar exchange rate (€_US$)	1.5 US $\cdot$ €$^{-1}$
Expected lifetime	15 years
Interest rate	6%
Plant availability	90%
Operators[a]	4[b] p./shift
Operator's salary	60'000 € $\cdot year^{-1}$
Wood costs (Φ_{wood}=50%)	33 € $\cdot MWh^{-1}$
O_2 costs (1-10$^5 m^3 \cdot h^{-1}$)(Kirschner, 2000)	0.02-0.5 € $\cdot kg^{-1}$
Electricity price (green)	180 € $\cdot MWh^{-1}$
Fuel sale price	120 € $\cdot MWh^{-1}$

[a] Full time operation requires three shifts per day. With a working time of five days per week and 48 weeks per year, one operator per shift corresponds to 4.56 employees.

[b] For a plant size of 20MW of biomass. For other production scales, an exponent of 0.7 with respect to plant capacity is used.

the Murphree efficiency.

5 Process Performance

5.1 Performance Indicators

The overall energy performance depends on the efficiency of the operations transforming the woody biomass into fuel and on the quality of the process integration. Whereas the former is related to the reactant stoichiometry, the type of product, the technology choice and its operating conditions, the latter depends on the appropriate choice of the energy conversion and distribution system, and the heat recovery system.

The overall energy efficiency ϵ_{tot} defined by Eq.17, takes into account the chemical energy available in the product, the energy available in the feedstock and the produced ($\dot{E}^-$) or consumed ($\dot{E}^+$) electricity, where thermal and mechanical energy are considered equivalent.

$$\epsilon_{tot} = \frac{\Delta h^0_{Fuel,out} \cdot \dot{m}_{Fuel,out} + \dot{E}^-}{\Delta h^0_{Biomass,in} \cdot \dot{m}_{Biomass,in} + \dot{E}^+} \tag{17}$$

A chemical efficiency ϵ_{chem} (Eq. 18) is defined based on the substitution of fuel equivalents for the consumed and by-produced power to assess the value of the products with respect to the technical feasibility of their further conversion into final energy services and competing technologies. The electricity fuel equivalent is calculated using an efficiency of 55%. All the reported efficiencies are expressed on the basis of the lower heating value of dry biomass.

$$\epsilon_{chem} = \frac{\Delta h^0_{Fuel,out} \cdot \dot{m}_{Fuel,out} + \frac{1}{\eta_{NGCC}} \frac{\Delta h^0_{SNG}}{\Delta k^o_{SNG}}(\frac{1}{\eta_{HP}}\dot{Q}^- + \dot{E}^-)}{\Delta h^0_{Biomass,in} \cdot \dot{m}_{Biomass,in}} \tag{18}$$

The economic performance is evaluated by the investment and the production costs, as described in section 4.3 and in Gassner and Maréchal (2009b).

The thermo-economic modeling approach is illustrated only for some process configurations and for different plant capacities of 20 and 400MW of biomass.

5.2 Process Integration Analysis

The influence of the heat recovery and the cogeneration systems including the steam network, the utilities and the introduction of supplementary equipments like gas turbines (GT) or heat pumps, on the process performance is analyzed.

5.2.1 Steam Network

The introduction of a Rankine cycle allows for recovering mechanical power from excess heat, while producing also the required process steam. Its performance depends on the number of steam production and utilization levels and the associated pressure or temperature (Maréchal and Kalitventzeff, 1997). If these are chosen in a correct way, the process performance is improved by a sound energy conversion. This influence is highlighted here by comparing three different configurations for the DME process: the first one ("none") refers to the situation where no steam cycle is integrated, "simple steam cycle " defines a setup with one single pressure level per cycle (6MPa) and "advanced steam cycle" defines a setup that includes two pressure levels for steam production (5&12MPa). In the advanced setup, the utilization levels correspond to the temperature of the gasification steam production, the steam requirement of the stripper of the MEA absorption unit and the cooling water temperature is used to define the condensation level. The numerical results are presented in Table 8 and the comparison of the composite curves for two different steam networks is illustrated in Figure 5. This shows how the implementation of an appropriate steam network may increase the overall thermo-economic performance. Through the additional mechanical power generated by the steam turbine, the energy efficiency is improved since the net electricity demand is decreased. The production costs decrease, even if the investment costs increase due to the purchase of the steam turbine.

Table 8: Mechanical power balance expressed in [kW of electricity per MW of biomass], energy and economic performance for a plant capacity of 20 and 400MW of biomass, for the DME process with air drying, directly heated CFB gasification, reforming at 850°C and cold gas cleaning for different steam network configurations.

Steam cycle		none	simple	advanced
Power Consumption [kW·MW^{-1}]	Process	138	138	138
Power Production [kW·MW^{-1}]	Steam Turbine	0	82	96
	Expansion Turbine [a]	7	7	7
Net electricity [kW·MW^{-1}][b]	Output	-131	-49	-35
Performance	ϵ_{tot} [%]	39.8	42.9	43.5
- Invest. [M€]	20 MW biomass	17.5	19.9	20.8
	400 MW biomass	246	264	273
- Prod. Cost [€·MWh^{-1}]	20 MW biomass	157	135	132
	400 MW biomass	130	105	102

[a] The pressurized offgases are expanded in a turbine to the burner pressure.

[b] The net electricity output expressed in kW of electricity per MW of biomass is negative when the integrated process requires additional electricity importation and positive when it generates electricity.

5.2.2 Heat Pump Integration

In the MeOH process, the implementation of a heat pump with an evaporation temperature of 378K and a condensation temperature of 428K using water as fluid can improve the quality of the energy integration. The mechanical vapor recompression from the absorber to the MEA stripper
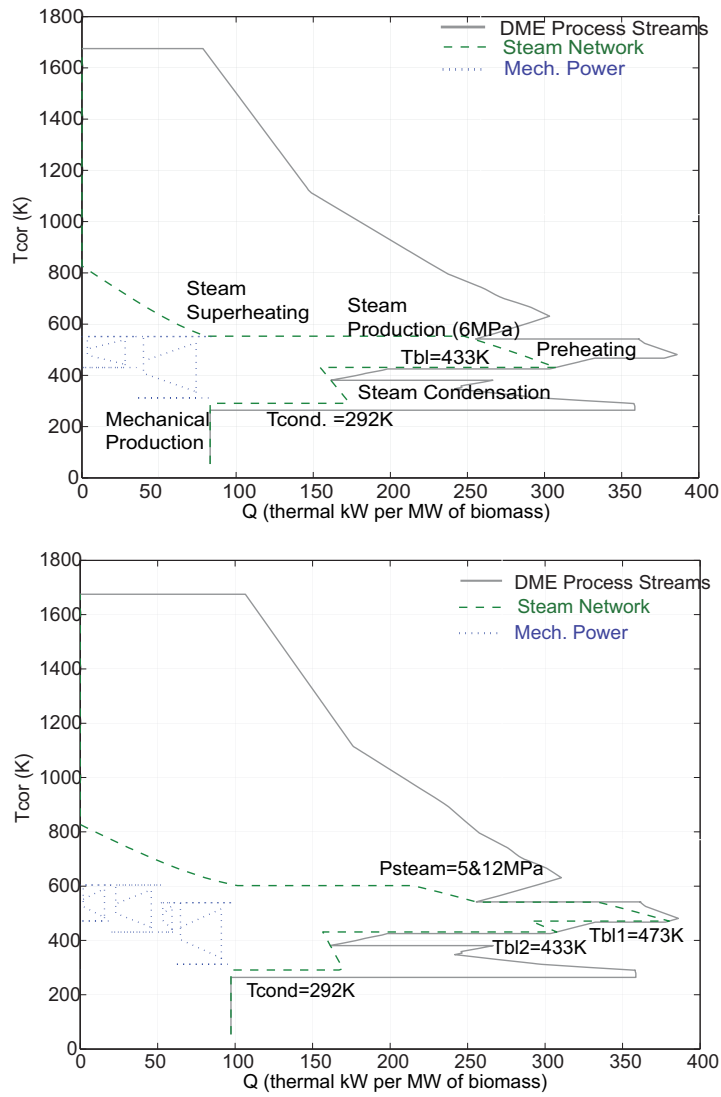
Figure 5: Integrated composite curves of the steam network for the DME process with air drying, directly heated CFB gasification, reforming at 850°C and cold gas cleaning. Top: simple steam cycle, bottom: advanced steam cycle.

reaches a coefficient of performance of 5.8. By reducing the need for steam at 1 bar it allows to convert the high temperature heat to mechanical power as illustrated on the composite curve of Figure 6. With this measure, the steam cycle coproduces 12 times more electricity per MW of biomass which reduces the net electricity consumption by 35%. For an additional investment of around 5.5%, the overall energy efficiency is increased from 50.8 to 52.3% and the production costs are decreased by 6 €·MWh^{-1} (4.2%) on fuel basis.

5.2.3 Gas Turbine

The process offgases can be used in a gas turbine in order to improve the combined heat and power integration. The gross power production from the excess energy of the DME-production process with directly heated CFB gasification is increased by around 12% due to this introduction of a gas turbine. As shown in Table 9, the net electricity consumption of the plant is decreased by 40%, which increases the overall energy efficiency and decreases the production cost by 4%
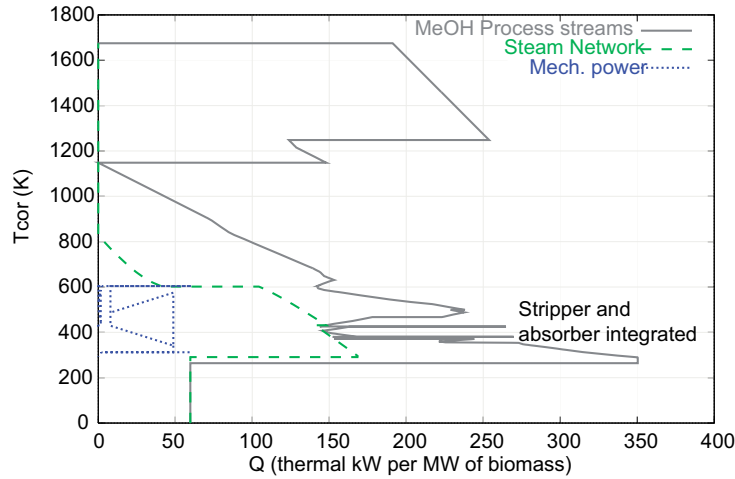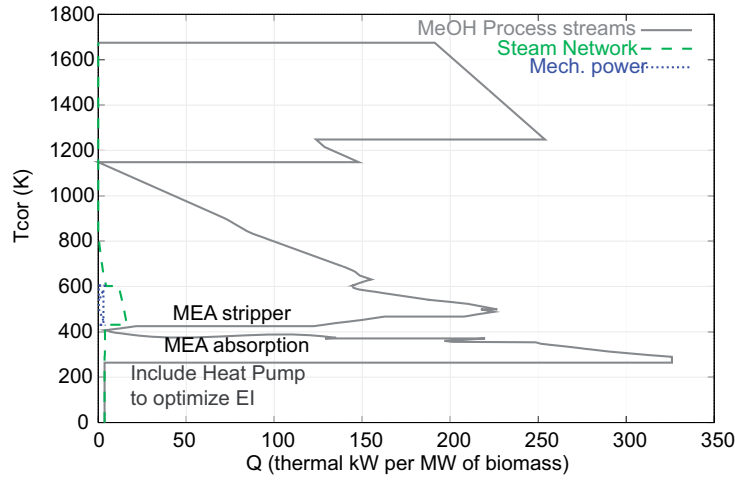
Figure 6: Analysis of the heat pump integration in the MeOH process with steam drying, FICFB gasification, reforming at 950^oC and cold gas cleaning without (top) and with the integration of a heat pump (bottom).

($5€·MWh^{-1}$ on fuel basis). A similar effect is also observed for the MeOH and FT-crude process with directly heated pressurized CFB gasification, whereas for the processes with indirectly heated gasification the performance is not further improved.

Table 9: Mechanical power balance expressed in [kW of electricity per MW of biomass], energy and economic performance for a plant capacity of 20 and 400MW of biomass, for the DME process with air drying, directly heated CFB gasification, reforming at 850°C and cold gas cleaning with and without gas turbine.

		Boiler	Gas Turbine
Power Consumption $[kW \cdot MW^{-1}]$	Process	138	138
Power Production $[kW \cdot MW^{-1}]$	Steam Turbine	96	65
	Expansion Turbine	7	0
	Gas Turbine	0	52
Net electricity $[kW \cdot MW^{-1}]$	Output	-35	-21
Performance	ϵ_{tot} [%]	43.5	44.2
- Invest. [M€]	20 MW biomass	20.8	21
	400 MW biomass	273	270
- Prod. Cost $[€·MWh^{-1}]$	20 MW biomass	132	128
	400 MW biomass	102	96

5.2.4 Steam Methane Reforming

Apart from the configuration of the cogeneration system, the overall performance of the conversion also depends on the operating conditions of the different process units. Their optimal values are thereby related to the quality of the energy integration of the plant, since the utility system is supplied with offgases and intermediate streams from the principal product conversion. The equilibrium of the steam methane reforming for the stoichiometric adjustment of the syngas is for example shifted by changing the reforming temperature or pressure or by adapting the steam to carbon ratio. This influences both the composition of the gases and the heat requirement. The impact of the temperature is studied in detail here, while the other parameters could be included in a multi-objective optimization. Since the steam reforming reaction is endothermal (Eq.11), more methane is formed at low temperature, while carbon monoxide and hydrogen are formed at higher temperatures. Accordingly, lower reforming temperature causes both the amount of heat and its temperature level to decrease, whereas higher temperature results in an increased heat demand at higher temperature. In FT-synthesis, methane as a first-order hydrocarbon is an undesired side-product and is not reformed. Higher methane content in the raw gas thus decreases the product yield in the FT-reactor and increases the amount of offgas that is produced. Thus, a trade-off between the methane conversion in the reforming and its heat demand is expected. This impact is shown in Figure 7 for different CO-conversions.
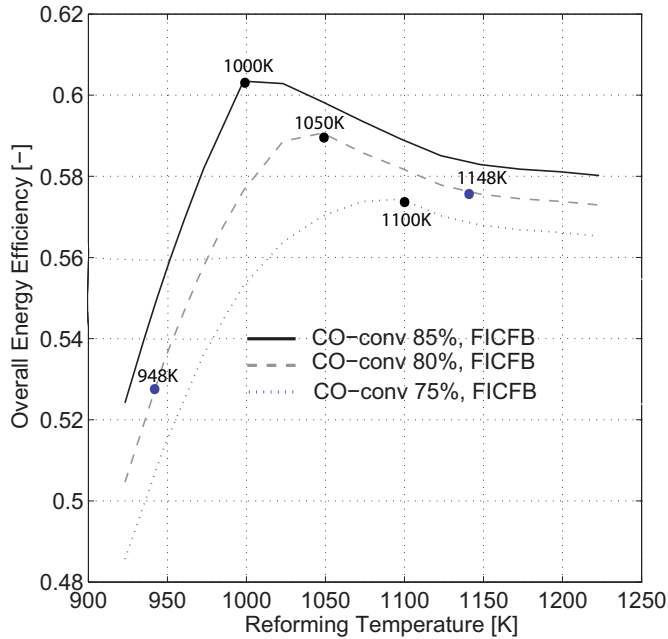

Figure 7: Influence of the reforming temperature [K] on the overall energy efficiency of the FT-crude process with air drying, CFB gasification (P=0.1MPa) indirectly heated and cold gas cleaning for different CO-conversions.

At low temperature, too much methane is present and the productivity of the FT-crude process drops, since the CH_4 cannot be reformed. With increasing temperature, less methane is present, the product yield of the synthesis and also the heat demand for the reforming are increased, and less offgases to supply this heat are remaining. Too high temperatures therefore result in an exaggerated reforming of methane, since reformed product gas must be burnt anyway to supply the necessary process heat.

17

As the energy potential of the offgas and syngas changes, the relative consumption of the intermediate product gas used as combustible and the corresponding quantity in absolute terms changes with the reforming temperature. This difference of the heat demands in the energy integration is depicted by comparing the composite curves for two selected reforming temperatures and for 80% CO-conversion on Figure 8.
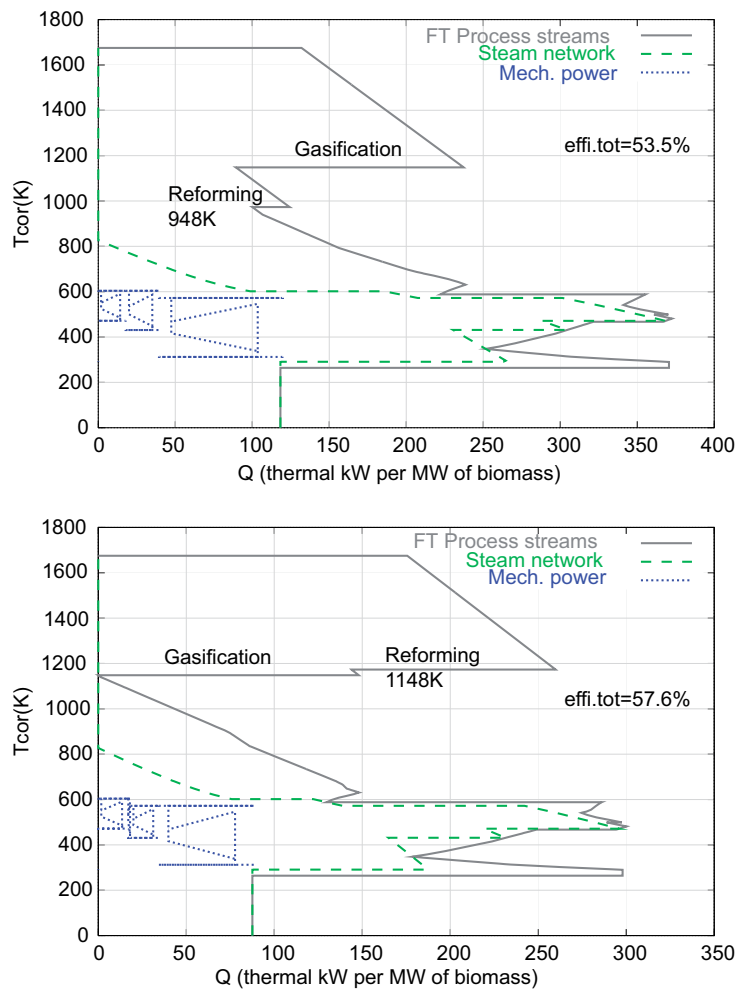

Figure 8: Comparison between the composite curves for two different reforming temperatures (top: 948K; bottom: 1148K) for the FT-crude process with air drying, FICFB gasification (P=0.1MPa), cold gas cleaning and CO-conversion of 80%.

Figure 9 shows that at low temperature no syngas is burnt, since the offgas contains a large amount of methane. In contrary, at higher temperature, part of the syngas has to be used to cover the heat demand because the energy potential of the offgas is not sufficient. As the sections upstream the reforming are not influenced, the absolute energy supply from the torrefaction gas and char are unchanged, and the relative share only changes due to the different total demand. The total amount of the energy to be supplied by the combustion of syngas and waste passes through a minimum at the optimal reforming temperature, at which the offgases are used and the heat demand and temperature of the endothermal reforming are kept low.
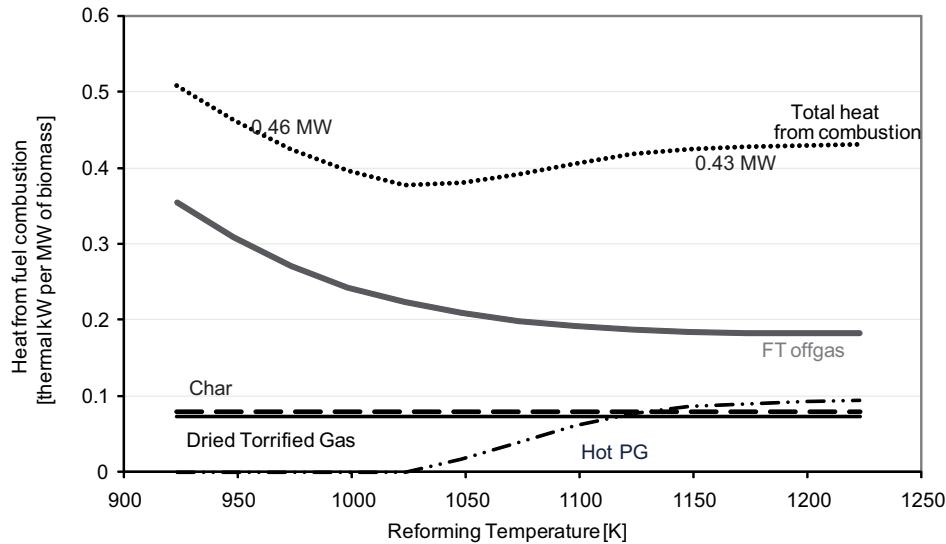
Figure 9: Relative and absolute thermal energy [MW per MW of biomass], supplied from the combustion of syngas, offgas and waste as a function of the reforming temperature of the FT-crude process.

The energy integration could be further improved by performing successive reforming steps at different temperatures. By performing a first steam methane reforming step below the pinch temperature and a second step above it, the total heat demand would be reduced, which further would increase the overall energy efficiency by 1.5 points and reduce the production costs of the FT-crude fuel by $1.3€·MWh^{-1}$ on fuel basis.

5.3 Thermo-economic process performance

The influence of technological process options is studied for some exemplary process configurations defined in Table 10. For these scenarios, adequate values of the key operating parameters were determined in preliminary sensitivity analysis. The studied configurations for the FT-crude process include indirectly (ind) and directly (d) entrained flow (FT-EF_ind & FT-EF_d) and fluidized bed gasification (FT-a & FT-c) with and without gas recycling (FT-a & FT-b). For the MeOH process two alternative technologies for CO_2 removal are considered the MEA process (MeOH-a & MEOH-c) and the Selexol process (MeOH-b & MEOH-d) for indirectly (MeOH-a & MEOH-b) and directly heated fluidized bed gasification (MeOH-c & MEOH-d), respectively.

5.3.1 Pretreatment and gasification options

For the different options, air drying and steam drying perform similarly in terms of efficiency, but in terms of investment air drying is more advantageous. Hot gas cleaning (HGCL) features slightly higher energy efficiency than cold gas cleaning (CGCL), some technical developments are however required to reach maturity.

Since the entrained flow gasification requires a pyrolysis step before gasification, a torrefaction unit is also included for all the other processes configurations for a coherent comparison. The exemplary comparison of the same technology scenarios with and without torrefaction for the FT-crude process with indirectly heated fluidized bed gasification shows only a slight performance difference. The heat and power demand of the torrefaction step reduces the power production by the steam network and consequently decreases the net electricity output by $5.7kW·MWh^{-1}$. However the chemical efficiency (ϵ_{chem}) is increased from 57.7% to 59.3% by an increased fuel production resulting from the modified gas composition prior to the synthesis

19

Table 10: Parameters choices, mechanical power balance expressed in [kW of electricity per MW of biomass], energy and economic performance for a plant capacity of 20 and 400MW of biomass, for the different options of the investigated FT, DME and MeOH processes (Heating mode: d=direct and ind=indirect).

Case	FT-EF_ind	FT-EF_d	FT-a	FT-b	FT-c	DME	MeOH-a	MeOH-b	MeOH-c	MeOH-d
					Process Parameters					
Synthesis	FT	FT	FT	FT	FT	DME	MeOH	MeOH	MeOH	MeOH
$P_{synthesis}$ [MPa]	2.5	2.5	2.5	2.5	2.5	5.0	8.5	8.5	8.5	8.5
$T_{synthesis}$ [°C]	340	340	340	340	340	277	260	260	260	260
Drying	air	air	air	air	air	air	air	air	air	air
Gasification type	EF	EF	CFB	CFB	FICFB	FICFB	FICFB	FICFB	CFB	CFB
Heating mode	ind	d	d	d	ind	ind	ind	ind	d	d
Reforming P [MPa]	-	-	3	3	0.1	0.1	0.1	0.1	3	3
Reforming T [K]	-	-	1050.15	1050.15	1050.15	1223.15	1223.15	1223.15	1623.15	1623.15
Gas Cleaning	cold	cold	cold	cold	cold	cold	cold	cold	cold	cold
CO_2 removal [%]	none	none	none	none	none	MEA	MEA	Selexol	MEA	Selexol
Gas Recyling [%]	0	0	0	80	0	80	90	90	90	90
H_2/CO	2	2	2	2	2	1.3	-	-	-	-
CO-conversion	85	85	85	85	85	-	-	-	-	-
Steam network:										
Production levels [MPa]	8&12	8&12	8&12	8&12	8&12	5&12	5&12	5&12	5&12	5&12
Utilization levels [K]	473&433	473&433	473&433	473&433	473&433	473&433	473&433	473&433	473&433	473&433
Condensation level [K]	292	292	292	292	292	292	292	292	292	292
					Mechanical Power Balance expressed in kW per MW of biomass					
Fuel Output $[kW \cdot MW^{-1}]$	637	458	303	352	601	561	570	570	318	318
Power Consumption $[kW \cdot MW^{-1}]$:										
PG production	20	33	25	25	22	22	22	22	34	34
Synthesis	0	0	0	0	65	71	92	71	14	0
CO_2 removal	0	0	0	0	0	11	27	34	35	12
O_2 supply	0	26	9	9	0	0	0	0	24	24
Total	20	59	34	34	87	104	141	127	107	70
Power Production $[kW \cdot MW^{-1}]$:										
Steam Turbine	0	106	179	153	76	50	43	55	80	96
Expansion Turbine	6	8	10	7	7	6	13	13	9	9
Net electricity $[kW \cdot MW^{-1}]$	-14	55	155	126	-4	-48	-85	-59	-18	35
					Energy Efficiency					
ϵ_{tot} [%]	62.8	51.3	45.8	47.8	59.8	53.5	52.5	53.8	31.2	35.3
ϵ_{chem} [%]	61.4	54.7	55.6	55.7	59.3	48.0	43.3	47.4	28.7	37.4
					Economic performance for a plant capacity of 20MW of biomass					
Investment [M€]	7	10	11	12	19	23	27	28	15	15
Investment Depreciation $[€ \cdot MWh^{-1}]$	8	14	24	22	21	27	31	33	31	32
Prod. Cost $[€ \cdot MWh^{-1}]$	68	76	70	75	89	113	128	123	159	135
Biomass break-even cost [a]$[€ \cdot MWh^{-1}]$	66	53	48	49	51	37	29	31	20	28
					Economic performance for a plant capacity of 400MW of biomass					
Investment [M€]	88	101	115	133	295	311	364	363	156	136
Investment Depreciation $[€ \cdot MWh^{-1}]$	5	7	13	13	17	19	21	21	16	14
Prod. Cost $[€ \cdot MWh^{-1}]$	54	50	33	43	72	90	103	96	116	88
Biomass break-even cost [a]$[€ \cdot MWh^{-1}]$	75	65	59	60	62	50	43	47	34	43

[a] The biomass break-even cost is expressed in € per MWh of biomass with a fuel sale price of 120 $€ \cdot MWh^{-1}$.

step. In the economic performance this improves the biomass break-even cost from 49.2 to 51.5 $€ \cdot MWh^{-1}$ on basis of 20MW of biomass.

The performances of the different gasification technologies for the FT-crude process are compared in Table 10. The indirectly heated entrained flow gasification (FT-EF_ind) potentially yields the highest performance but the technical realization of such a process operating at high temperature and being heated indirectly has yet to be proven. For the directly heated EF gasification process (FT-EF_d) the efficiency is lower by around 11.5 points to 51.3% when compared with the FT-EF_ind option .

The indirectly heated fluidized bed gasification (FT-c) outperforms in terms of overall energy efficiency the directly heated gasification (FT-a) in a process with a reforming step at the same temperature. Directly heated CFB gasification has a lower fuel efficiency, because of the stoichiometry of the syngas being less suited for FT-synthesis. However, its pressurized operation allows for eliminating the syngas compression prior to synthesis and more electricity is generated by the steam turbines from the process excess heat. More net electricity is therefore produced and the production costs are thereby reduced by around 15% due to the benefit from the electricity exportation for the directly heated CFB gasification. There is a certain trade-off

between both terms of the thermo-economic performance. The biomass break-even cost reflects the benefits of the indirectly heated gasification that produces much more fuel. The power balance represented in Figure 10 illustrates the benefit in terms of compression power for the pressurized gasification and the power consumption related to the oxygen supply.
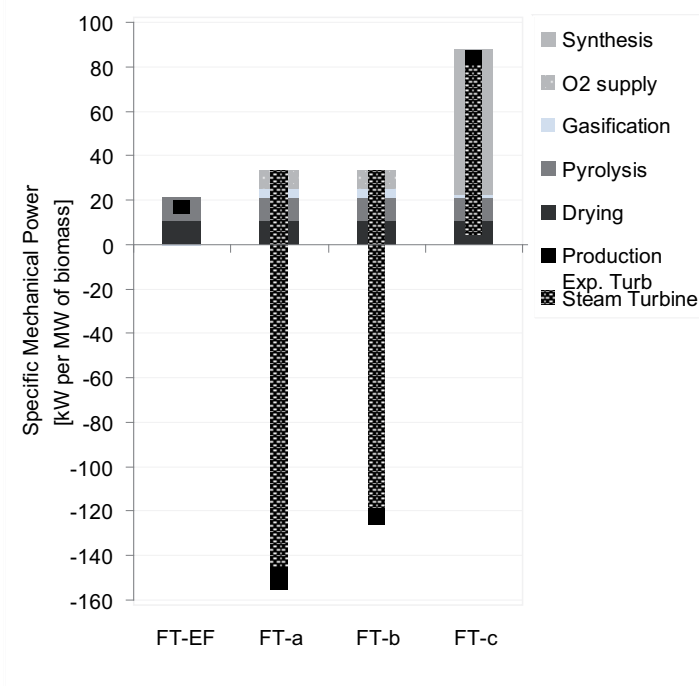

Figure 10: Mechanical power balance, including power consumption and production, expressed in [kW of electricity per MW of biomass] for the investigated FT-crude processes (Table 10) with indirectly heated entrained flow (EF) and directly (FT-a, FT-b) or indirectly (FT-c) heated fluidized bed gasification.

The difference in process efficiency due to the heat integration is illustrated in Figure 11.

The FICFB features a pinch point at high temperature that specifies the burner fuel consumption. In the directly heated cases, the required heat for gasification is provided by partial oxidation of the syngas and the energy content of the synthesis residues can not be used for gasification. Consequently, less chemical energy is contained in the syngas and more heat is available for power cogeneration. In (Tijmensen et al., 2002) it was reported for a similar once through FT concept with 80% conversion and direct, oxygen blown, pressurized gasification an overall energy efficiency of 47.8% and a nearly 10 points lower efficiency for the indirect, air-blown, atmospheric gasification (38.9%). The opposed trend found here can be explained by the benefits of the detailed process integration.

By recycling 80% of the unreacted gas (FT-b), the overall energy efficiency is increased from 45.8% to 47.8%, but this reduces the power output significantly and increases the production cost by 5-10 €·MWh^{-1} on fuel basis. Compared to a similar configuration studied in (Hamelinck et al., 2004), the FT-crude process with gas recycling has a higher energy efficiency: 47.8% compared to 36-40%[2]. This difference is again attributed to the benefit of the process integration.

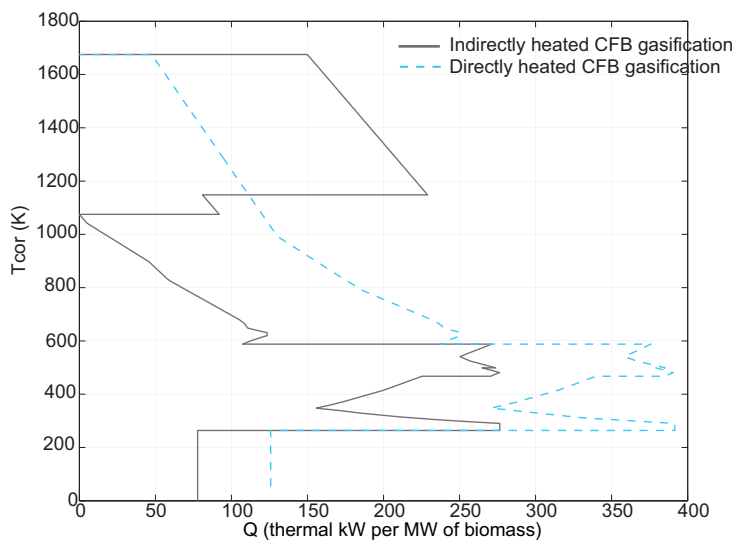[2]efficiency expressed on the higher heating value basis.

Figure 11: Composite curves including a steam network (for clarity not shown on the figure) for indirectly and directly heated fluidized bed gasification for the FT-crude process without gas recycling (FT-a and FT-c) with air drying and cold gas cleaning.

It is interesting to note that for the SNG production studied in (Gassner and Maréchal, 2009b) the directly heated gasification yield higher performance, since for the indirectly heated gasifier syngas needs to be burnt to balance the energy requirement as only few offgas is available.

5.3.2 Synthesis Options

The difference in the performance of the three fuel production processes is highlighted in Table 10 by comparing the results for the same upstream process options (FT-c, MeOH-a and DME). In this comparison the higher efficiency of the FT-crude process is partly explained by the fact that in the FT-crude process no CO_2 removal unit is needed before the synthesis because no stoichiometry adjustment is required, and that the FT-upgrading is not considered in this study, the final product being the crude FT-fuel.

The comparison of the composite curves in Figure 12 depicts some important differences between the energy integration of these processes.

The change in the plateau length representing the exothermal synthesis reactions results from the different heat of reaction. In the DME and MeOH process, the CO_2 removal by chemical absorption with MEA is a large heat sink influencing the energy integration and the combined heat and power generation and hence the overall efficiency. Although the chemical conversion is increased by CO_2 removal, its heat requirement limits the electricity cogeneration and its beneficial effect on the process economics. Alternative methods for CO_2 removal driven by partial pressure differences and consuming almost no heat such as physical absorption (i.e. Selexol or Rectisol process (Burr and Lyddon, 2008)) could improve the process performance. The Selexol process removes the heat demand at lower temperature and increases the electricity coproduction, as highlighted by the scenarios for the MeOH production defined in Table 10. By replacing the MEA absorption step with the Selexol absorption in the case of pressurized gasification (scenarios MeOH-c and MeOH-d), the net power output can be increased by a factor of 2.8 and consequently the overall energy efficiency can be increased from 31.2 to 35.3%, while the production costs are decreased by 15%. For the atmospheric gasification (scenarios MeOH-a and MeOH-b) the performance is only increased from 52.5 to 53.8% because of the syngas
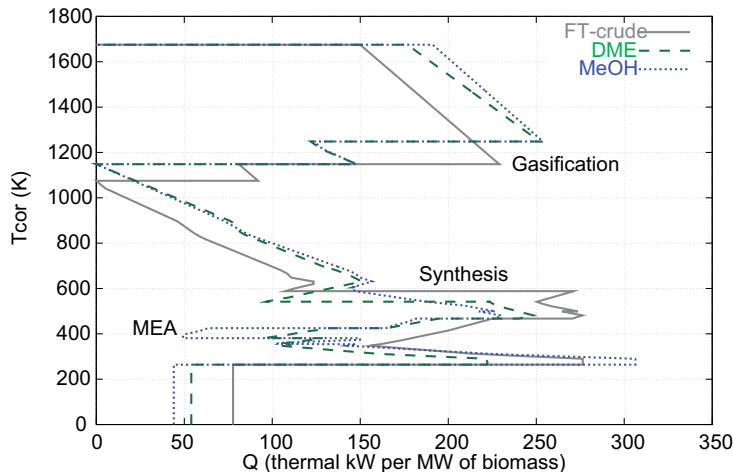
22

Figure 12: Composite curves for the different investigated synthesis processes (FT-c, MeOH-a, DME) (Table 10).

compression requirement. For the MeOH process, the comparison of the gasification technology leads to the same conclusions as for the FT-crude process. The results show a nearly 20 points higher overall efficiency for the indirectly heated gasification due to the higher fuel production.

The difference in the economic performance of the three synthesis processes illustrated in Table 10 and Figure 13 and is related essentially to the variation in the power balance. Since the operating pressures of the synthesis reactions are different, the power requirement for the compression and hence the electricity purchase costs differ considerably. The power consumption is the highest for the MeOH process operated at 8.5MPa. The investment costs of the MeOH and DME processes are furthermore increased by the additional costs of the CO_2 removal unit. The comparison of the biomass break-even cost shows that at the assumed fuel sale price there is only an advantage to produce MeOH by this process if biomass is available at a relative low price.

A detailed analysis of the economic performance presented in Figure 13 reveals that the gasification represents around 40% of the investment. Compared to the ECN results (Hamelinck et al., 2004; Hamelinck and Faaij, 2002), the investments found for a plant capacity of 400MW are around 40% higher for the methanol plant and in the same range for the FT plant without upgrading. Contrary to their approach, the investment estimation method applied here rates the equipment with conventional design heuristics that take the operating conditions into account. As pilot plant data are used as reference for the design parameters, it can be expected to yield realistic figures. The production costs are formed in average about 44% by the raw material cost, 25% by the investment, 21% by the maintenance and 10% by the electricity cost. Consequently, further progress and development in the field of biomass gasification technology could decrease the investment. Large scale productions, optimized cogeneration systems and efficient raw material conversion by high-performance catalysts are also expected to increase the economic competitiveness. Other technological developments and progress that could potentially increase the competitiveness of the liquid fuel production processes from biomass are the on-site production of oxygen by oxygen selective membranes instead of oxygen supply and the technical realization of indirectly heated entrained flow gasification. Moreover, the economic performance depends highly on the biomass and the electricity prices, which is illustrated by the sensitivity analysis results reported in Table 11 for two different prices.
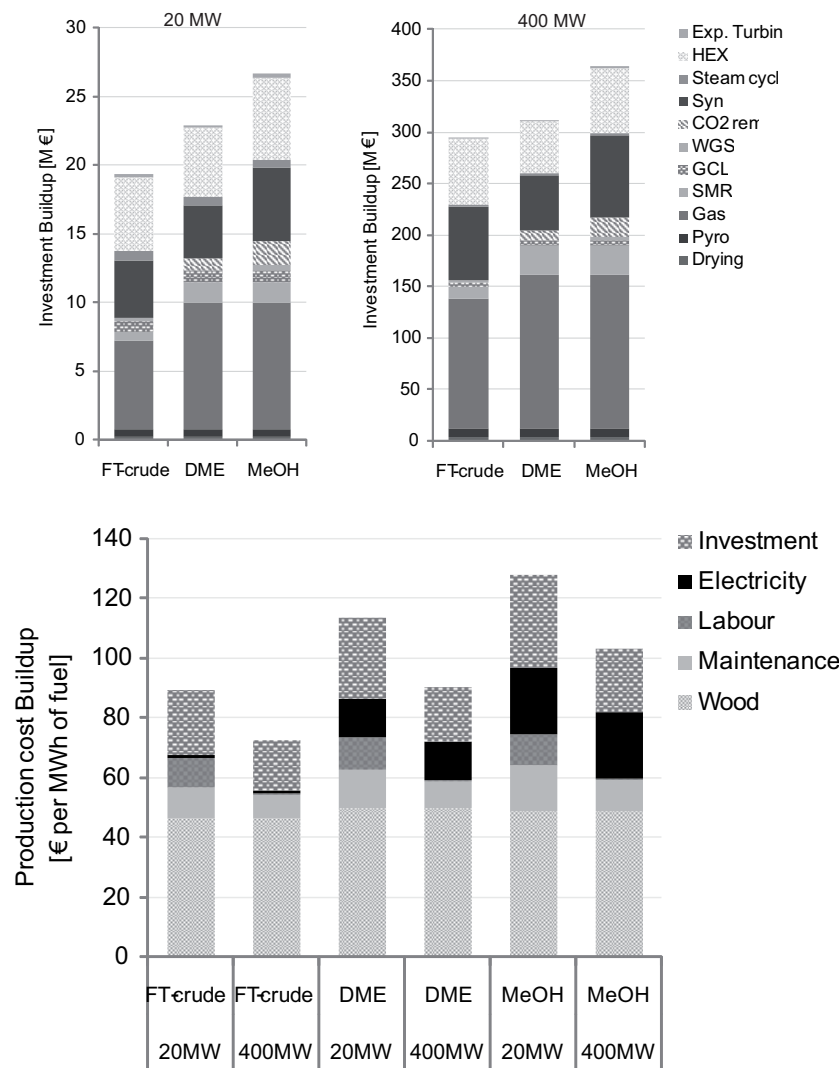
Figure 13: Economic performance expressed by the buildup of the investment [M€] (top) and the total production cost in [€ per MWh of fuel] (bottom) calculated with the assumptions of Table 7 for the different synthesis processes defined in Table 10 (FT-c, DME and MeOH-a) for a plant capacity of 20 and 400 MW of biomass

.

6   Conclusion

In this paper, a superstructure-based thermo-economic model for candidate processes to produce liquid fuels from lignocellulosic biomass has been presented with the purpose to evaluate their competitiveness systematically with regard to the efficiency of the energy integration and the economic performances. The flowsheet models are developed based on literature data from existing industrial and pilot installations. These models are expected to accurately predict the performances of the process and consequently to identify promising system configurations that could lead to a detailed design of the optimal plant. The energy integration defines the optimal

Table 11: Sensitivity analysis results of the electricity and biomass price influence on the economic performance of the different synthesis processes defined in Table 10 (FT-c, DME and MeOH-a) for a plant capacity of 20MW and 400MW of biomass

Parameter	FT		MeOH		DME	
Electricity price [€·MWh^{-1}]	120	230	120	230	120	230
Biomass price [€·MWh^{-1}]	20	45	20	45	20	45
	Economic performance for a plant capacity of 20MW of biomass					
Biomass break-even cost [€·MWh^{-1}]	49	54	31	27	37	37
Prod. Cost [€·MWh^{-1}]	70	106	101	151	89	134
	Economic performance for a plant capacity of 400MW of biomass					
Biomass break-even cost [€·MWh^{-1}]	60	64	45	41	50	50
Prod. Cost [€·MWh^{-1}]	53	88	76	126	66	111
	Production cost build-up					
Investment [%]	31[a](31)[b]	20 (19)	31 (28)	21 (17)	31 (28)	20 (17)
Labour & Maintenance [%]	29 (16)	19 (10)	25 (14)	17 (9)	27 (14)	18 (9)
Wood [%]	39 (52)	59 (70)	29 (38)	43 (52)	33 (45)	50 (60)
Electricity	1 (1)	1 (2)	15 (19)	19 (23)	9 (13)	12 (15)

[a] Production cost build-up for a plant capacity of 20MW of biomass.

. [b] Production cost build-up for a plant capacity of 400MW of biomass.

choice of utilities and maximizes the combined heat and power production and allows to analyze options for waste streams valorization. The improvement of the process performance due to an appropriate energy integration is investigated in detail. The developed process models are appropriate for a future thermo-economic optimization according to the methodology presented in (Gassner and Maréchal, 2009a) and for the evaluation of the environmental impacts through a detailed life cycle analysis by applying the methodology described in (Gerber et al., 2009).

The performance computation for the different process options yields overall efficiencies in the range of 50 to 60%. The most critical choice defining the performance is the choice of the gasification technology. In contrast to the results reported in (Tijmensen et al., 2002), the best configuration includes indirectly heated circulating fluidized bed gasification followed by steam methane reforming. Although oxygen-blown, pressurized CFB-gasification is the best option for SNG-production (Gassner and Maréchal, 2009b), the synthesis of liquid fuel suffers from an important amount of unconverted offgas that is readily used for indirectly heating of the gasifier. Besides the technology choice, the operating conditions of the process unit operation and primarily the quality of the energy integration highly influence the process performance. The optimization of a combined cycle valorizing the waste heat in the power production increases the overall energy efficiency. With the assumptions made in this study including different plant capacities and the scenarios for the raw materials and energy prices, the production costs for the different processes reach a level in the range of respectively 53-106 €·MWh^{-1} on fuel basis for the FT-crude process, 76-151 €·MWh^{-1} for the MeOH process and 66-134 €·MWh^{-1} for DME process (Table 11). When compared with fuel market prices, the corresponding biomass break-even costs are in the range of 49-64, 27-45 and 36-50 €·MWh^{-1} on biomass basis for the FT, MeOH and DME process respectively. In the long term, the competitiveness of these biofuels on the energy market can increase, since costs improvements due to larger production scales, technological learning and development in gasification technology and increased conversion efficiencies through improved catalysts can be expected.

References

Burr, B., Lyddon, L., 2008. A comparison of physical solvents for acid gas removal. Tech. rep., Bryan Research & Engineering, Bryan, Texas, USA.

DECHEMA, Last visited 07/2009.
URL `http://www.dechema.de/`

ECN, Last visited 07/2009. Energy Research Centre of the Netherlands: Biomass, Coal and Environmental Research.
URL `http://www.ecn.nl/en/bkm/`

Fiedler, E., Grossmann, G., Kersebohm, D., Weiss, G., Witte, C., 2000. Methanol. In: Ullmann's Encyclopedia of Industrial Chemistry. Wiley-VCH.

Fox, J. M., Degen, B. D., Cady, G., Deslate, F. D., Summers, R. L., (Bechtel Group, Inc.), 1990. Slurry reactor design studies: Slurry vs. fixed-bed reactors for Fischer-Tropsch and methanol: Final report. Tech. rep., US. Department of Energy.

Gassner, M., Maréchal, F., Mar. 2009a. Methodology for the optimal thermo-economic, multi-objective design of thermochemical fuel production from biomass. Computers & Chemical Engineering 33 (3), 769–781.

Gassner, M., Maréchal, F., 2009b. Thermo-economic process model for the thermochemical production of Synthetic Natural Gas (SNG) from lignocellulosic biomass. Biomass & Bioenergy 33 (11), 1587–1604.

Gerber, L., Gassner, M., Maréchal, F., 2009. Integration of LCA in a thermo-economic model for multi-objective process optimization of SNG production from woody biomass. In: Proc. 19th European symposium on CAPE. Vol. 1. Elsevier, Amsterdam, pp. 1405–1410.

Gmehling, J., Onken, U., 1988. Vapor-Liquid Equilibrium Data Collection, Aqueous systems Supplement 2. Vol. Vol I, Part 1b. DECHEMA Chemistry Data Series, Frankfurt am Main.

Gmehling, J., Onken, U., 2005. Vapor-Liquid Equilibrium Data Collection, Alcohols: Methanol Supplement 5. Vol. Vol I, Part 2g. DECHEMA Chemistry Data Series, Frankfurt am Main.

Grambezen, P. V., -. Contribution à l'étude cinétique de la synthése du méthanol par le procédé industriel sous basse pression. Tech. rep., Ecole militaire Bruxelles.

Hamelinck, C. N., Faaij, A. P. C., Sep. 2002. Future prospects for production of methanol and hydrogen from biomass. Journal of Power Sources 111 (1), 1–22.

Hamelinck, C. N., Faaij, A. P. C., den Uil, H., Boerrigter, H., Sep. 2004. Production of FT transportation fuels from biomass; technical options, process analysis and optimisation, and development potential. Energy 29 (11), 1743–1771.

Jager, B., Espinoza, R., 1995. Advances in low temperature Fischer-Tropsch synthesis. Catalysis Today 23 (1), 17–28.

Kaneko, T., Derbyshire, F., Makino, E., Gray, D., Tamura, M., 2001. Coal Liquefaction. In: Ullmann's Encyclopedia of Industrial Chemistry. Wiley-VCH.

Kirschner, M. J., 2000. Oxygen. In: Ullmann's Encyclopedia of Industrial Chemistry. Wiley-VCH.

Maréchal, F., Heyen, G., Kalitventzeff, B., May 1997. Energy savings in methanol synthesis: Use of heat integration techniques and simulation tools. Computers & Chemical Engineering 21 (Supplement 1), S511–S516.

Maréchal, F., Kalitventzeff, B., Sep. 1997. Identification of the optimal pressure levels in steam networks using integrated combined heat and power method. Chemical Engineering Science 52 (17), 2977–2989.

Maréchal, F., Kalitventzeff, B., May 1998. Process integration: Selection of the optimal utility system. Computers & Chemical Engineering 22, 149–156.

Maréchal, F., Palazzi, F., Godat, J., Favrat, D., 2005. Thermo-Economic modelling and optimisation of fuel cell systems. Fuel Cells 5 (1), 5–24.

Ogawa, T., Inoue, N., Shikada, T., Ohno, Y., 2003. Direct Dimethyl Ether Synthesis. Journal of Natural Gas Chemistry 12, 219–227.

Ohno, Y., 2001. Development of DME direct synthesis technology. Tech. rep., DME Project-JFE Holding.

Olofsson, I., Nordin, A., Söderlind, U., 2005. Initial review and evaluation of process technologies and systems suitable for cost-efficient medium-scale gasification for biomass to liquid fuels. Tech. rep., Energy Technology & Thermal Process Chemistry, University of Umea.

Radgen, P., Cremer, C., Warkentin, S., Gerling, P., May, F., Knopf, S., 2005. Verfahren zur CO2-Abscheidung und -Speicherung. Abschlussbericht Forschungsbericht 20341110 UBA-FB 000938, Frauenhofer-Institut für Systemtechnik und Innovationsforschung, Bundesantstalt für Geowissenschaften und Rohstoffe.

Spath, P., Dayton, D., 2003. Preliminary screening-technical and economic assessment of synthesis gas to fuels and chemicals with emphasis on the potential for biomass-derived syngas. Tech. Rep. NREL/TP-510-34929, National Renewable Energy Laboratory, Colorado.

Tijmensen, M. J. A., Faaij, A. P. C., Hamelinck, C. N., van Hardeveld, M. R. M., Aug. 2002. Exploration of the possibilities for production of Fischer Tropsch liquids and power via biomass gasification. Biomass and Bioenergy 23 (2), 129–152.

Turton, R., 2009. Analysis, Synthesis, and Design of Chemical Processes, 3rd Edition. Prentice Hall, Upper Saddle River, N.J.

Ulrich, G., Vasudevan, P., 2003. A Guide to Chemical Engineering Process Design and Economics a Practical Guide, 2nd Edition. CRC, Boca Raton, Fla.

Wyer, S. S., 1907. A treatise on producer gas and gas-producers, 2nd Edition. Hill, New York.

Appendix - Supplementary material

Parameters of thermodynamic models

In the flowsheet modeling different thermodynamic models are used to calculate the liquid-vapor and chemical equilibrium. For the pretreatment units and the production of the syngas, ideal gas behavior has been selected. Ideal behavior is also assumed for the FT-crude process streams because of the presence of hydrocarbons. However, for the synthesis and purification units of the DME and MeOH routes the effects of binary interactions should be considered. The liquid and vapor phase behavior is predicted by the Peng-Robinson equation of state. The corresponding parameters of the Peng-Robinson model are obtained from DECHEMA Chemistry Data Series (Gmehling and Onken, 2005, 1988; DECHEMA, Last visited 07/2009) (Table 12).

The thermodynamic model used to calculate the interaction properties in the purification section is the activity coefficient model UNIQUAC for the methanol process and the NRTL model for the DME process. The parameters for each model are adapted from the DECHEMA Chemistry Data Series (DECHEMA, Last visited 07/2009) and reported in the following Tables 13, 14 & 15.

Table 12: Interaction parameters for the Peng-Robinson model adapted from DECHEMA Chemistry Data Series (Gmehling and Onken, 2005, 1988).

Peng-Robinson model		
Compound i	Compound j	kij
N_2	MeOH	-0.2141
C_2H_6	MeOH	0.027
H_2O	MeOH	-0.0778
CO	MeOH	-0.2141
CO_2	MeOH	0.0583

Table 13: Binary parameters for the activity at infinite dilution (Ln(gam)=isGAM0+isGAMT/T) in the UNIQUAC model for the MeOH separation adapted from DECHEMA Chemistry Data Series (DECHEMA, Last visited 07/2009).

UNIQUAC model			
Compound i	Compound j	isGAM0	isGAMT
CH_4	H_2O	5.41	-0.25
CH_4	MeOH	6.2	0
N_2	H_2O	3.0	0
N_2	MeOH	3.0	0
H_2O	CO	6.96	0
H_2O	CO_2	8.69	-1543.5
H_2O	H_2	7.96	0
CO	MeOH	2.9	0
CO_2	MeOH	0.99	-121.85
H_2	MeOH	4.7	0

Table 14: Coefficients for the UNIQUAC equation for the free energy for the MeOH separation unit adapted from DECHEMA Chemistry Data Series (DECHEMA, Last visited 07/2009). The parameters Aij, Bij, Aji, Bji occur in the relationships (Uij - Ujj) / R = Aij + Bij / T and (Uji - Uii) / R = Aji + Bji / T where Uij, Ujj, Uji and Uii are the coefficients from the UNIQUAC equation for free energy and R is the perfect gas constant. Here temperature independency is assumed: Bij=Bji=0.

UNIQUAC model			
Compound i	Compound j	Aij	Aji
H_2O	MeOH	239.67	-153.37
H_2O	EtOH	178.14	-31.03
MeOH	EtOH	-6.039	-1.79
MeOH	DME	-145.46	433.94

Table 15: Coefficients from the NRTL equation for the free energy for the DME separation unit (adapted from DECHEMA Chemistry Data Series (DECHEMA, Last visited 07/2009)). The NRTL parameters ijC0, ijCT, jiC0, jiCT, ijA0, ijAT are involved in the relationships (gij-gjj) / R = ijC0 + ijCT· T, (gji-gii) / R = jiC0+jiCT·T and Aij=ijA0+ijAT·T where gij, gji, gii, gjj and Aij are the coefficients from the NRTL equation for the free energy and R is the perfect gas constant. Here temperature independency is assumed: ijCT=jiCT=ijAT=0.

NRTL model				
Compound i	Compound j	ijC0	jiC0	ijA0
H_2O	DME	567.58	-284.52	0.3
H_2O	MeOH	-86.60	386.75	0.3
DME	MeOH	187.80	-66.27	0.3